

# A new principle in design of composite materials: reinforcement by interlocked elements

A.V. Dyskin<sup>a,\*</sup>, Y. Estrin<sup>b</sup>, A.J. Kanel-Belov<sup>c</sup>, E. Pasternak<sup>a</sup>

<sup>a</sup>Department of Civil and Resource Engineering, The University of Western Australia, 35 Stirling Hwy, Crawley, WA 6009, Australia

<sup>b</sup>Institut für Werkstoffkunde und Werkstofftechnik, Technische Universität Clausthal, Agricolastr. 6, D-38678 Clausthal-Zellerfeld, Germany

<sup>c</sup>Youth Centre of Science and Technology, B. Vlasievsky 11, Moscow, 119002, Russia

Received 19 June 2001; accepted 29 May 2002

## Abstract

We propose a new materials design concept based on the use of regular assemblies of topologically interlocked elements. A particular implementation of this concept, viz. a layer of tetrahedron-shaped elements, was studied in some detail. The packing arrangement in the layer is such that each individual element is held in place by its immediate neighbours. This structure can provide a load-bearing skeleton of a composite material. A second phase, serving as a matrix or binder, can be selected to provide special structural or functional properties such as thermal or sound insulation, fluid transport, controlled electrical conductivity, etc. It is envisaged that strong and flexible composite materials with high impact resistance can be created on this basis. A model specimen assembled according to this topological principle was tested with respect to its stiffness and load bearing capacity. First experimental and theoretical results show that a layer consisting of many interlocked elements has a much larger mechanical compliance than its monolithic counterpart, and can withstand considerable deformations. Other possible shapes of three-dimensional elements interlocked into a monolayer and the principles of their generation are discussed. The design principle proposed opens up new avenues for creating multifunctional composite materials.

Crown Copyright © 2002 Published by Elsevier Science Ltd. All rights reserved.

**Keywords:** A. Particle-reinforced composites; B. Layered structures; B. Fracture; B. Stress–strain curves; Interlocked structures

## 1. Introduction

In a recent communication [1], a new material architecture was proposed based on regular assemblies of identical interlocked elements. Owing to the topology of packing, an individual ‘building block’ is held in place by its immediate neighbours without the aid of friction or adhesion. We believe that the possibility of producing such topologically ‘self-locked’ assemblies opens a new direction in design and manufacturing of special strong and flexible composite materials with high impact resistance. While the interlocked elements form a skeleton structure that can provide structural integrity of a composite, a second phase can be selected to satisfy specified functional requirements, e.g. with regard to electrical or thermal conductivity, sound attenuation,

etc. Since the properties of the assemblies are determined by its topology, rather than by the size of the ‘building blocks’, the topologically motivated materials design principle proposed can be used in large scale engineering structures, as well. In the present paper, we explore some mechanical properties of materials whose design is based on the principle of topological interlocking.

The idea of using interlocking building blocks, e.g. interlocking bricks [2], in civil engineering has been around for quite some time. However, the known methods of interlocking are based on the use of connectors, which lead to undesirable stress concentrations. Our alternative approach makes use of the topological possibility of establishing self-locking in assemblies of simple convex shaped elements, thus avoiding stress concentrators. This idea was realised in a layer structure consisting of identical tetrahedron-shaped elements packed in a special way. Some interesting findings of the first mechanical tests done on an experimental assembly with the proposed architecture that were reported in [1]

\* Corresponding author. Tel.: +61-8-9380-3987; fax: +61-8-9380-1044.

E-mail address: [adyskin@cyllene.uwa.edu.au](mailto:adyskin@cyllene.uwa.edu.au) (A.V. Dyskin).

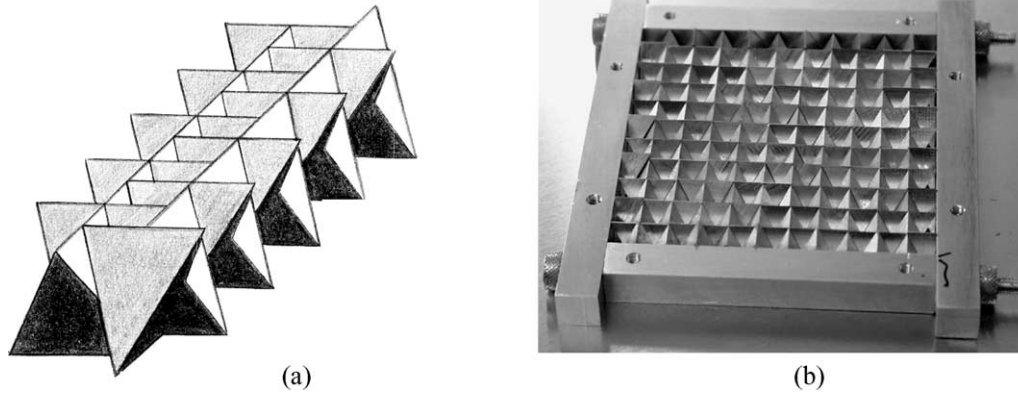


Fig. 1. Assembly of interlocked tetrahedrons: (a) the principle of topological interlocking [1]; (b) view of the actual assembly in a special rigid frame restricting its lateral movement.

are reviewed. Theoretical considerations regarding deformation and failure of this type of assembly are considered. Finally, further classes of topologically interlocked architecture are proposed.

## 2. Self-locking assembly of tetrahedral

The architecture based on packing of identical tetrahedra that was proposed and described in [1] is shown in Fig. 1.<sup>1</sup> While in this assembly a tetrahedron embedded in the structure, i.e. surrounded by at least three neighbours, cannot be removed by movement in any direction, including the vertical one, the tetrahedra at the periphery of the assembly can be removed by lateral movement. Hence, the structure as such cannot withstand strains in the lateral directions, i.e. the in-plane strains. However, when placed in a confinement at its periphery, Fig. 1b, an assembly of this kind will preserve its structural integrity without any adhesive or connectors.

## 3. Bearing capacity and stiffness of the assembly

To implement the above materials design concept in a real specimen, an assembly of 100 interlocked tetrahedra was produced. The tetrahedra with the edge length of  $a=1$  cm were made from a commercial Al–Mg–Si alloy and were used in the as-machined condition. The assembly was placed in a rigid steel frame, Fig. 2, which was tightened to hold the structure in place. The boundary rows of elements consisted of halves of regular tetrahedra. The assembly was loaded in an Instron machine by a cylindrical indenter 1 cm in diameter.

Fig. 3 shows the force vs. indenter displacement diagram. For comparison, the results for the same kind of



Fig. 2. Concentrated force loading of the self-locking assembly. Lateral movement of tetrahedrons is restricted by a rigid frame ('clamped boundary condition').

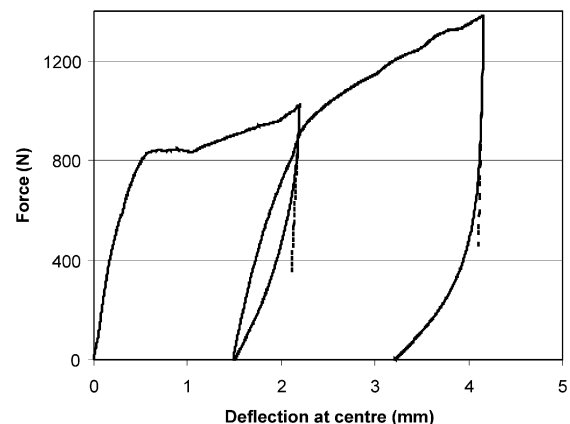


Fig. 3. Force vs. deflection diagram for the assembled layer: loading and unloading curves, clamped edge conditions. (Note an intermediate unloading from about 1000 N with subsequent reloading.) Straight broken lines indicate the gradient of the first and second unloading.

<sup>1</sup> When the paper was submitted we learned that similar arrangement of tetrahedral was considered by Glickman [3] as a basis of a new pavement design.

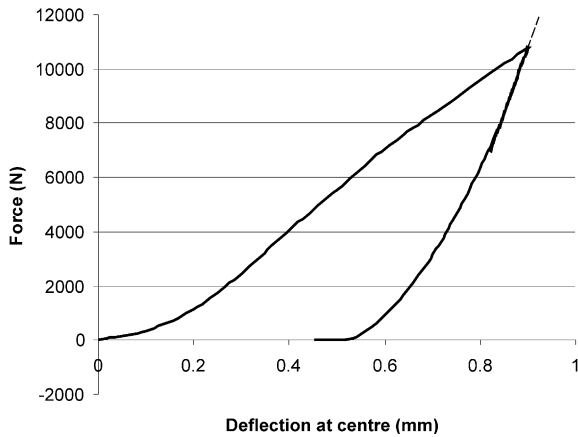


Fig. 4. Force vs. deflection diagram for the reference solid plate with simply supported edges: loading and unloading curves. Straight broken line indicates the gradient of the unloading.

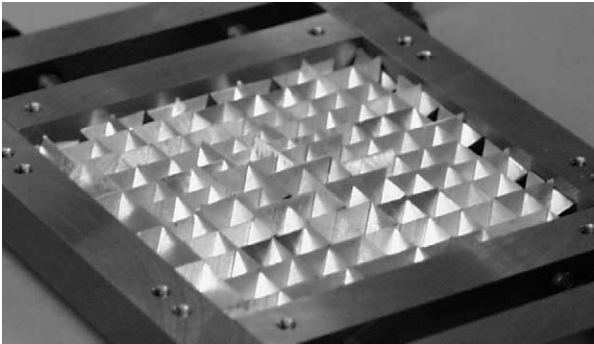


Fig. 5. The assembly after unloading.

loading of a solid plate from the same material and of the same thickness as the assembled layer ( $a/\sqrt{2} \cong 0.71$  cm) are shown in Fig. 4. The comparison was made on the basis of equal thickness because the bending of plates is controlled by the flexural rigidity that strongly depends upon the thickness. (Note that simply supported loading, rather than the clamped boundary condition, was used in testing the reference plate.) To measure the bending stiffness (flexural rigidity), the unloading curves were recorded as well. The unloading curve for the assembly shows that the nearly elastic component is fairly non linear. The residual deformation upon total unloading is very pronounced (Figs. 5 and 6). The fact that the individual tetrahedra, even in the most heavily loaded central part of the structure showed no sizeable plastic deformation suggests that the residual (irreversible) displacement of the tetrahedra forming a dome-shaped indent (Fig. 6) is associated with collective behaviour of the assembly.

A comparison of the unloading curves in Figs. 3 and 4 demonstrates that the initial slopes of the first and the second unloading curves (16.2 and 17.7 kN/mm, respectively) are by a factor of about 3 smaller than the slope for the solid reference plate (48.7 kN/mm). The difference in the effective stiffness between the assembly and the solid plate was estimated in [1]. The different boundary conditions imposed in these two cases had to be taken into account, of course. While the assembly was loaded with the periphery clamped, the solid plate was simply supported. The difference was evaluated by modelling both objects as disks of the same radius  $R$  loaded with a concentrated force,  $F$ , applied at the

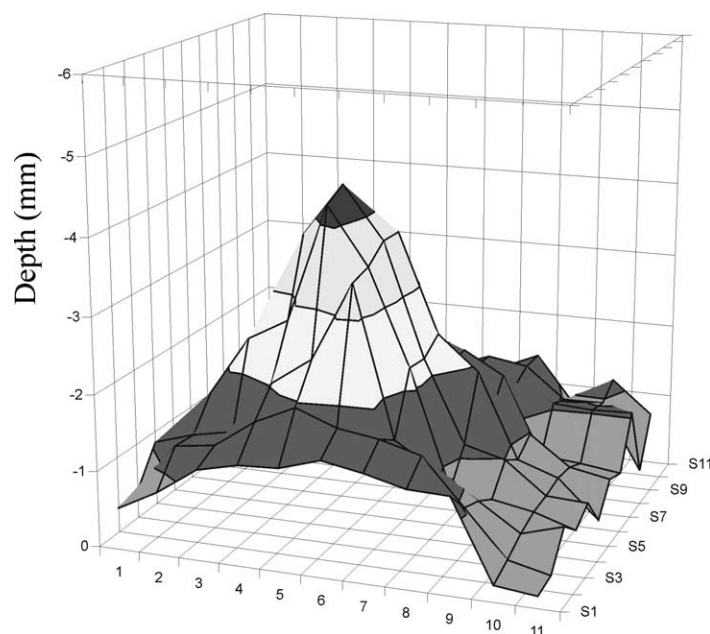


Fig. 6. Profile of the assembly after unloading.

centre. An analytical solution available for that case, e.g., [4], yields for the plate bending stiffness:

$$D = \frac{1}{16\pi} \frac{F}{u} R^2 \psi, \quad (1)$$

where  $u$  is the deflection at the centre and the factor  $\psi$  depends on the boundary conditions ( $\psi = 1$  and  $\psi = (3 + \nu)/(1 + \nu)$  for the case of clamping and simple support, respectively, with  $\nu$  denoting Poisson's ratio). The disc radius was 'gauged' by comparing  $D$  given by Eq. (1) for simply supported solid plate with a formula expressing  $D$  in terms of the plate thickness  $h$ , viz.  $D = Eh^3/12(1 - \nu^2)$  [4]. With Young's modulus  $E = 70$  GPa and  $\nu = 0.34$  the value of  $R = 3.11$  cm was obtained—somewhat larger than the radius of a circle inscribed in the specimen (2.75 cm). The value of bending stiffness for the solid plate is 2.33 kNm. With the data shown in Fig. 3 it follows for the assembly  $D = 0.31$  kNm and  $D = 0.34$  kNm (as determined from the first and the second unloading curves, respectively). It is seen that the bending stiffness of the assembled layer is almost an order of magnitude smaller than that of a solid plate of the same thickness.

Fig. 5 shows the assembly plate after unloading, while Fig. 6 shows its measured profile (the assembly was actually turned upside down to produce the photograph and the profile). It is friction between the blocks that prevents them from returning to their initial position. Thus, the structure exhibits large residual (macroscopic) deformations, which suggests a possibility of using processes similar to metal forming to form a plate into a desirable shape.

It is remarkable that despite a lack of any binder phase, the load bearing capacity of the assembled structure is fairly high (of the order of 1 kN). It should

also be mentioned that in addition to translational degrees of freedom, the elements possess rotational ones. Tilting of the adjacent tetrahedra towards the indenter during the loading eventually leads to a contact between them. This gives rise to additional frictional resistance to penetration.

#### 4. Mechanism of low bending rigidity

An obvious explanation for the low bending stiffness of the assembly is the reduced contact area between the blocks. The contact surface is a rhombus with the side length  $a/2$ , Fig. 7a, inclined to the normal to the assembly plane at an angle equal to  $\cos^{-1}\sqrt{2/3}$ . After projection onto a plane perpendicular to the plane of the assembly, the contact surface assumes the form depicted in Fig. 7b. By identifying the area of this contact surface with the cross-sectional area of an 'equivalent' solid body, the cylindrical bending stiffness can be calculated as

$$D = \frac{Ea^3}{192\sqrt{2}(1 - \nu^2)} \quad (2)$$

For a solid plate of the same thickness as the assembled layer ( $a/\sqrt{2}$ ) one has

$$D = \frac{Ea^3}{24\sqrt{2}(1 - \nu^2)} \quad (3)$$

Thus, the values of the bending stiffness differ by exactly a factor of 8. The obtained ratio is close to the values following from Figs. 3 and 4 (7.5 and 6.9 for the first and second unloading, respectively; see [1] for details).

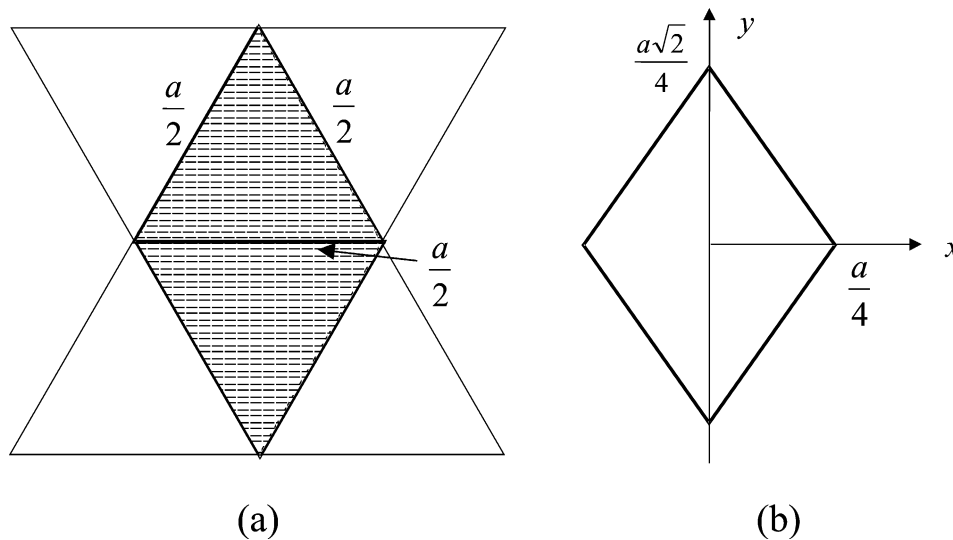


Fig. 7. Contact area between adjacent tetrahedrons of size  $a$ : (a) actual contact area; (b) projection of the contact area onto a plane normal to the assembly plane.

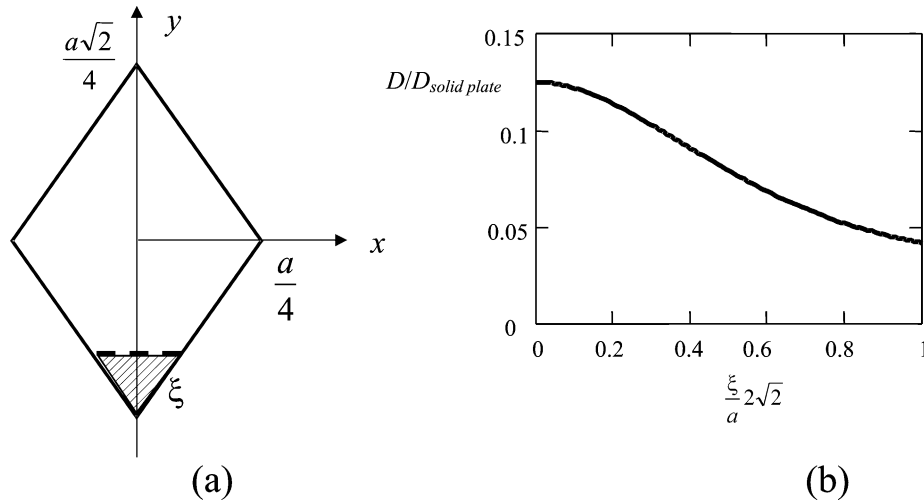


Fig. 8. The influence of delamination area (joint) caused by bending-induced tensile stress: (a) delamination area (joint); (b) cylindrical bending stiffness vs. joint height.

## 5. Discussion

### 5.1. Non-linearity of force–displacement curve

The bending stiffness computed in the previous section characterises the deformation of assembly with full contact between the blocks. Bending under concentrated force loading produces local tensile stresses (in the experiment discussed the maximum stress is at the bottom surface of the assembly). These stresses are counterbalanced by the compressive stresses created by the restraining frame until the bending becomes such that the maximum tensile stress reaches the magnitude of the compressive stress. Since the blocks are not glued together, further loading will result in a joint between adjacent blocks. The joint in its projection on the direction normal to the assembly plane is shown in Fig. 8a by shadowed area. Fig. 8b shows the ratio between the bending stiffnesses of the assembly and the reference solid plate as a function of the height  $\xi$  of the joint projection. The reduction of the bending stiffness demonstrated by the plot is a mechanism of the observed non-linear deformation. More detailed analysis of the tests would require the information about the lateral compression induced by the restraining frame.

### 5.2. Possible mechanisms of failure of assemblies of interlocking elements

The results of the tests and the analysis reported demonstrate that assemblies of interlocked tetrahedron-shaped elements are capable of withstanding considerable local (macroscopic) plastic deformation without losing their structural integrity. This suggests that such assemblies can possess great energy absorbing capacity and, possibly, high resistance to local impact. Applications as protective layers or coatings are envisaged,

especially if efficient ways of manufacturing and assembling small size tetrahedra are found. With the view of such applications, possible mechanisms of failure of a tetrahedron assembly due to impact should be considered.

Suppose an impact resulted in failure of a single block. Fig. 9 shows an assembly with a missing block (marked by white broken line), which is found to retain its integrity. From this one can conclude that the occurrence of a single ‘vacancy’ is not sufficient for disintegration of the layer. Therefore, failure of an assembly should be associated with breakage of a certain number of blocks. Two extreme cases can be considered: (a) *long distance propagation of a crack* initiated in one block and (b) *distributed fracturing of blocks* caused by an external action such that blocks fail at random and *accumulation of independently failed blocks* can be assumed [5].

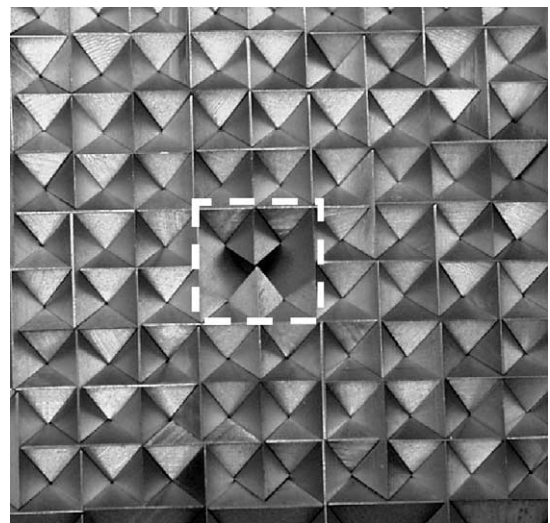


Fig. 9. Assembly of tetrahedrons with a missing block (indicated by white broken line).

Long distance crack propagation requires growth of a crack generated in a particular block into adjacent blocks. However, as the blocks are not strongly connected to each other, a mechanism similar to Cook-Gordon crack retardation [6] should be expected to operate (see also [7,8] for analysis of crack crossing frictional interfaces). This mechanism is illustrated in Fig. 10 where, for the sake of simplicity, a mode I crack in a fractured block propagating normal to the interface is shown. At a distance  $r$  from the crack tip the crack creates normal tensile stress  $\sigma_x = K_I(2\pi r)^{-1/2}$  (e.g., [6]). As the crack tip approaches the interface, the magnitude of this stress increases. Eventually it becomes sufficient to split part of the structure open at the interface (if there is no adhesion between the blocks) or create an interface void. This interface void/crack acts to reduce the stress concentration at the tip of the primary crack, which leads to arresting the primary crack. Propagation of fracture into the adjacent block is thus prevented. Therefore, it is the *weak adhesion* of the blocks (or total lack thereof in a single-phased interlocked assembly) that isolates a failed block and preserves the integrity of the assembly. Only when the compressive stress acting normal to the interface and the friction are considerably high, the crack will be able to cross the interface ([8]) and propagate into the neighbouring block.

Accumulation of independently failed blocks will now be considered as a possible mechanism of failure. Since

an individual missing or failed block cannot cause overall failure of the assembly, the accumulation of missing or failed blocks needs to form a connected chain for the assembly to start disintegrating. If one considers connectivity of failed blocks as the overall failure criterion and also assumes that the blocks are destroyed at random, failure should be attributed to the concentration of failed blocks reaching the percolation threshold. In the case under consideration, where the blocks form a square lattice, one has to deal with the so-called *site problem* [9], Fig. 11, since each block has four neighbours (Fig. 11a) and its failure would lead to the removal of support it lends to its neighbours. Therefore, in this respect the assembly can be modelled by a square lattice, the removal of a site corresponding to block failure, Fig. 11b. For the site problem on a square lattice, the percolation threshold was shown to be 0.59 [9]. That is to say, for the case of random block failure, around 59% of the blocks need to be destroyed for an assembly to completely lose its integrity.

The above consideration ignored a possibility of forming loops of broken blocks. As soon as sufficiently large loop is formed, the blocks within the loop will fall and the whole assembly will start disintegrating. Therefore the percolation threshold presents an upper estimate for the number of broken blocks needed to cause the collapse of the assembly.

This estimate also shows that assemblies are possible in which a large percentage of blocks are replaced with

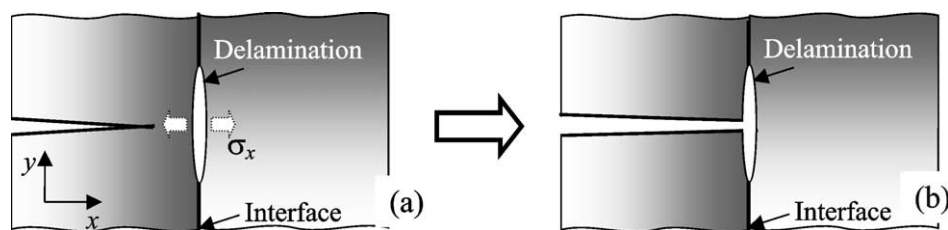


Fig. 10. Mechanism of crack retardation: (a) crack propagation from a fractured block towards an interface. Concentration of tensile stress acting in the direction of crack propagation creates interface delamination; (b) the delamination eventually arrests the propagation of the primary crack.

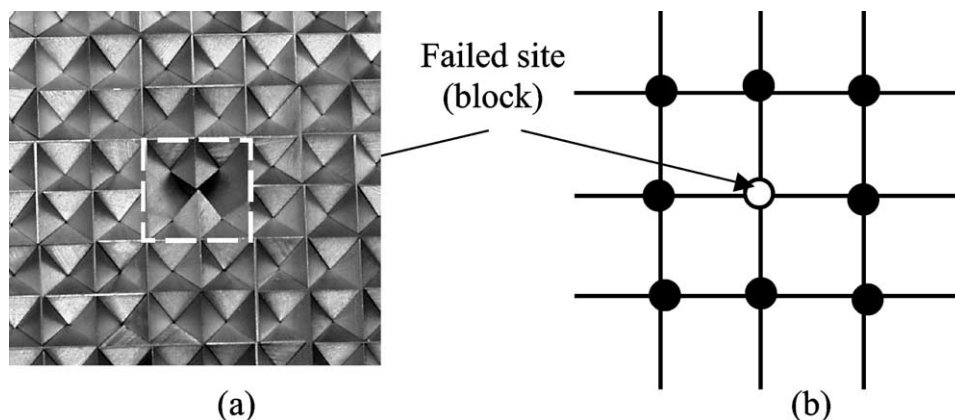


Fig. 11. Percolation model of failure of an assembly due to random block destruction: (a) assembly of tetrahedrons with a missing block (indicated by white broken line; this block was in contact with four neighbours); (b) the model: 2-D site percolation on square lattice.

blocks with the same geometry, but made from a different material that can be chosen to have desired functional properties. If this percentage is below the percolation threshold, the assembly will still maintain its structural integrity, regardless of the mechanical strength of the second phase.

Another remark is also due here. It is known that brittle materials exhibit the size effect—reduction in strength with increase in size of the loaded area of the material (in some cases the size effect is described by the Weibull statistics). When the material in question is replaced by an assembly consisting of interlocking blocks, its strength can be increased due to the size effect. Indeed, the elements of this fragmented structure are small and therefore stronger than a piece of solid material of the same size. Since fracturing of a single element does not yet causes failure of the structure, the weakest link concept is no longer applicable and thus the overall strength of the structure will not be decreased.

### 5.3. Multilayer structures

The proposed assembly is essentially layer-like. These layers can, however, be combined in multi-layer structures. Such structures will be characterised by reduced density and low stiffness. Indeed, simple geometric considerations show that the mass of an assembly of interlocking tetrahedra is only 2/3 of the mass of the solid reference plate. In the case of a low density matrix (or binder), or in the absence of a binder phase, the density of the composite will be close to 2/3 of the density of the bulk material. Combined with the inter-block gaps, the ‘porosity’ inherent in an engineered composite structure will lead to a considerable further reduction in the overall (macroscopic) elastic moduli. As a first approximation, the reduction in the moduli can be estimated by replacing the pyramidal gaps with spherical pores of the same volume fraction, i.e. 1/3. In this approximation, the effective moduli will remain isotropic. They can be determined by the differential self-consistent method (e.g. [10]). According to the method [10] the effective elastic moduli of a porous medium are obtained as a solution of the following system of differential equations

$$\begin{cases} \frac{dE_{\text{eff}}}{dv} = -2\pi E_{\text{eff}} \frac{(1 - \nu_{\text{eff}})(9 + 5\nu_{\text{eff}})}{7 - 5\nu_{\text{eff}}} \\ \frac{d\nu_{\text{eff}}}{dv} = 2\pi \frac{(1 - \nu_{\text{eff}}^2)(1 - 5\nu_{\text{eff}})}{7 - 5\nu_{\text{eff}}} \\ dp = \frac{4\pi}{3}(1 - p) \\ E_{\text{eff}}|_{p=0} = E, \nu_{\text{eff}}|_{p=0} = \nu \end{cases} \quad (4)$$

where  $E_{\text{eff}}$ ,  $\nu_{\text{eff}}$  are Young’s modulus and Poisson’s ratio of the porous material and  $p$  is porosity. This system

can be simplified by using Bruner’s [11] approximation according to which the values of slowly changing functions of  $\nu_{\text{eff}}$  in the right hand sides of the first two equations of (4) are replaced with their values at  $\nu_{\text{eff}}=0$ . This leads to the following simplified set of equations:

$$\begin{cases} \frac{dE_{\text{eff}}}{dv} = -\frac{18}{7}\pi E_{\text{eff}} \\ \frac{d\nu_{\text{eff}}}{dv} = \frac{2}{7}\pi(1 - 5\nu_{\text{eff}}) \\ dp = \frac{4\pi}{3}(1 - p)dv \\ E_{\text{eff}}|_{p=0} = E, \nu_{\text{eff}}|_{p=0} = \nu \end{cases} \quad (5)$$

Its solution has the form

$$E_{\text{eff}} = E(1 - p)^{27/14}, \quad \nu_{\text{eff}} = 0.2 + (\nu - 0.2)(1 - p)^{15/14} \quad (6)$$

For  $p = 1/3$  one has  $E_{\text{eff}}/E \sim 0.46$ , which is a reduction in Young’s modulus by about a factor of two. The effective Poisson’s ratio for  $\nu = 0.34$  is  $\nu_{\text{eff}} = 0.29$ . It should be noted that the effective Poisson’s ratio is very sensitive to the shape of the pores and therefore the approximation by spherical pores cannot be considered as very reliable for quantitative Poisson’s ratio calculations.

### 5.4. Further topologically interlocking shapes

Tetrahedra are not the only shapes that exhibit topological interlocking, although they are the simplest ones. Fig. 12a shows planar sections of the tetrahedron-based assembly giving a clue to a method of constructing other shapes. The middle section of the assembly consists of squares completely covering the area of the section. As the plane of the section moves away from the middle, the squares transform to rectangles oriented normally to each other. As the section plane continues to move away from the middle, the rectangles become thinner and longer and eventually degenerate into lines coinciding with the tetrahedron edge. It is this transformation of the central squares into longer rectangles that ensures interlocking. Indeed, consider a central block in Fig. 12a. The upper sections of its neighbours being long rectangles do not leave enough space for the middle section of the central block to go through when one attempts to remove the tetrahedron from the assembly by moving it upwards. This property is local since any even infinitesimally thin layer cut out from the assembly around its middle section would possess the same interlocking property. Therefore, the tetrahedra with two opposite edges machined away (Fig. 12b) also possess the interlocking property (Glickman [3] calls these blocks the G-blocks). The assembly from such

‘truncated’ tetrahedra will resemble the one shown on Fig. 1 after machining parallel to the assembly plane on both sides.

In the assembly considered the middle section consists of squares. From this point of view, the tetrahedron and truncated tetrahedron assemblies can be called square-

based. If the squares are replaced with some other symmetrical figures, e.g., octagons, a new group of shapes can be obtained. The only requirement is that as the section plane progressively moves away from the middle plane, the base figure transforms to the one with a continuously increasing aspect ratio. As this transformed

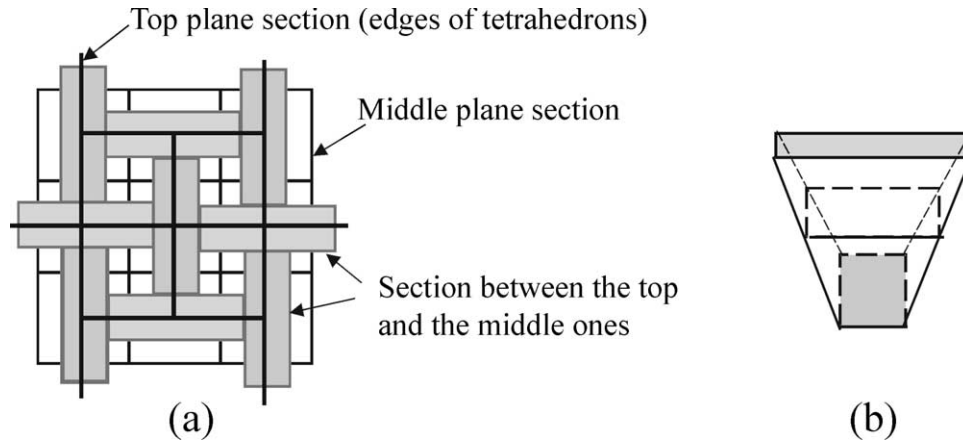


Fig. 12. Square-based assemblies: (a) planar sections of assembly of tetrahedrons; (b) a tetrahedron with two opposite edges cut away.

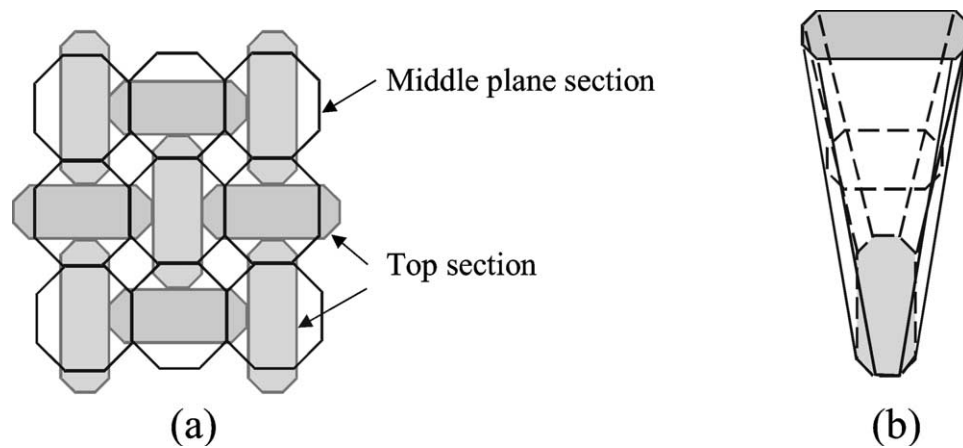


Fig. 13. Octagon-based interlocking shapes: (a) planar sections; (b) a pyramid with two opposite edges cut away.

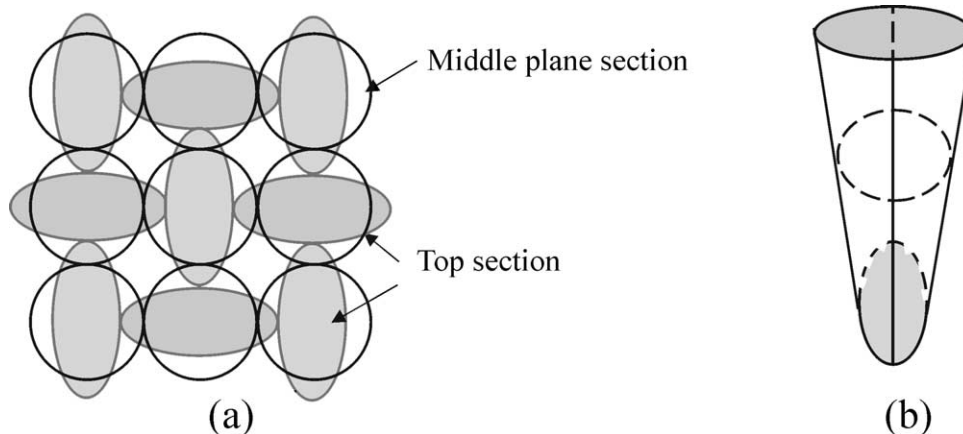


Fig. 14. Circle-based interlocking shapes: (a) planar sections; (b) an element.

figure represents the corresponding cross-section of the open ‘channel’ between the neighbours of an element, and the base figure is not able to pass through this opening, the element as a whole is locked in its position. This is illustrated by Fig. 13, which shows two planar sections of an octagon-based assembly (Fig. 13a) and the shape of an individual element (Fig. 13b). One can obviously keep doubling the number of sides of the base (middle plane) figures until a circle-based assembly is obtained as a limit, Fig. 14. A distinctive feature of such assemblies is their high porosity and permeability.

## 6. Conclusions

The proposed assembly of interlocked tetrahedron-shaped elements forms a layer in which each individual block is held in place by the neighbouring blocks. The layer is flexible, but can withstand considerable loads even if no binder is used to hold the elements together. The high flexibility of the layer is a result of reduced contact area between the neighbouring tetrahedra.

Failure of a single block cannot cause failure of the assembly as a whole, as with a single missing or destroyed block interlocking within the assembly is still retained. Weak adhesion between the blocks (or total absence of adhesion) leads to arrest of propagating cracks, induced e.g. by impact, and prevents them from spreading into neighbouring blocks. Therefore, the only way to break an assembly is to destroy a certain number of connected blocks. For block failure occurring at random and in an uncorrelated way, the total assembly disintegration will require fracturing of about 59% of all blocks.

The middle section of an assembly consists of a periodic array of squares. If the squares are replaced with some other symmetrical figures, e.g., octagons, a new class of shapes can be obtained.

Great opportunities are seen in finding processing routes for manufacturing such self-locking structures with different dimensional scales depending on the desired application. A further promising development would be by applying the novel materials design concept proposed to creating combinations of interlocked skeleton structures with appropriately chosen binder phases. Combinations of ceramic or metallic tetrahedron-shaped elements with polymeric binders are an obvious group of materials to look at in light of the above concept.

The demonstrated topological feasibility of producing self-locking assemblies is seen as a guideline to creating engineered flexible composite materials of high strength, fracture toughness and impact resistance. Further studies of new topologically viable architectonics of composites that would provide the desired self-locking are expected to open up new avenues in materials design.

## Acknowledgements

We wish to thank Karin Estrin for encouragement and advice on some aspects of this work. Discussions with Han Chuan Khor, Adrien Alla, Philip Howell and Oliver Nelson are also appreciated. Technical assistance of Uwe Hanke and Gerd Neuse is gratefully acknowledged.

## References

- [1] Dyskin AV, Estrin Y, Kanel-Belov AJ, Pasternak E. A new concept in design of materials and structures: Assemblies of interlocked tetrahedron-shaped elements. *Scripta Materialia* 2001;44: 2689–94.
- [2] Anand KB, Ramamurthy K. Development and performance evaluation of interlocking-block masonry. *J Architectural Engng* 2000;6(2):45–51.
- [3] Glickman M. The G-block system of vertically interlocking paving. In: *Second International Conference on Concrete Block Paving*, Delft, 10–12 April 1984. p. 345–8.
- [4] Landau LD, Lifshitz EM. *Theory of elasticity*. London; Reading (Ma): Pergamon Press and Addison-Wesley; 1959.
- [5] Estrin Y, Dyskin AV, Kanel-Belov AJ, Pasternak E. Materials with novel architectonics: assemblies of interlocked elements. In: Karihaloo BL, editor. *IUTAM Symposium on Analytical and Computational Fracture Mechanics of Non-Homogeneous Materials*. Dordrecht: Kluwer Academic; 2002. p. 51–5.
- [6] Parton VZ. *Fracture mechanics. From theory to practice*. Philadelphia: Gordon and Breach Science; 1992.
- [7] Dollar A, Steif PS. A tension crack impinging upon frictional interfaces. *J Appl Mech* 1989;56:291–8.
- [8] Renshaw CE, Pollard DD. An experimentally verified criterion for propagation across unbounded frictional interfaces in brittle, linear elastic materials. *Int J Rock Mech Min Sci Geomech Abstr* 1995;32(3):237–49.
- [9] Shklovskii BI, Efros AL. *Electronic properties of doped semiconductors*. Springer series in solid-state sciences, no. 45. Berlin: Springer-Verlag; 1984.
- [10] Vavakin AS, Salganik RL. Effective elastic characteristics of bodies with isolated cracks, cavities, and rigid nonhomogeneities. *Mechanics of Solids* 1978;13(2):87–97.
- [11] Bruner WM. Comment on ‘Seismic velocities in dry and saturated cracked solids’ by Richard J. O’Connell and Bernard Budiansky. *J Geophys Res* 1976;81(14):2573–6.